Proceedings World Geothermal Congress 2000
Kyushu - Tohoku, Japan, May 28 - June 10, 2000

THEORETICAL FEASIBILITY STUDIES OF RESERVOIR MONITORING USING GEOPHYSICAL SURVEY TECHNIQUES

John Pritchett[1], Jeffry Stevens[1], Philip Wannamaker[2], Shigetaka Nakanishi[3] and Shigeyuki Yamazawa [4]
[1]Maxwell Technologies Inc., 8888 Balboa Ave., San Diego, California 92123-1506, USA
[2]Energy and Geosciences Institute, University of Utah, 423 Wakara Way, Salt Lake City, Utah 84108, USA
[3]Electric Power Development Co., Ltd., 6-15-1 Ginza, Tokyo 104, Japan
[4]New Energy and Industrial Technology Development Organization, 3-1-1 Higashi Ikebukuro, Tokyo 170, Japan

Key Words: reservoir monitoring, numerical simulation, microgravity, resistivity, seismic, self-potential

ABSTRACT

A steady-state three-dimensional model of a hypothetical (but realistic and typical) geothermal reservoir system was developed using a numerical reservoir simulator. The region covers 81 square kilometers and extends to three kilometers depth. Under natural-state conditions, a shallow water/steam region underlies the central part of the anomaly, but the reservoir is otherwise liquid-dominated. Next, a reservoir exploitation strategy was devised, and enough fluid was produced and injected to operate a 50 MW geothermal power station, causing underground pressures, temperatures and steam saturations to evolve. Then, various mathematical "postprocessors" were applied to this computed 27-year reservoir history to appraise changes that might be observable using various surface measurement techniques. Methods examined include microgravity surveys, electrical resistivity surveys (both DC resistivity and MT surveys), self-potential (SP) surveys and seismic surveys. The results suggest that these techniques have considerable promise. By supplementing conventional data sets usually employed in reservoir engineering studies, they offer the potential to improve the quality of mathematical reservoir models, thereby permitting more accurate forecasts of reservoir performance, facilitating efficient reservoir management, and reducing the costs of geothermal electricity.

1. INTRODUCTION

The New Energy and Industrial Technology Development Organization (NEDO – a Japanese Government agency) has carried out various projects over the years to promote geothermal development. Starting in 1997, NEDO undertook a new initiative: *Development of Technology for Reservoir Mass and Heat Flow Characterization,* which is broadly divided into two parts: (1) *Characterization of the Hydrological Properties of Fractures* and (2) *Monitoring and Modeling of Reservoir Mass and Heat Flows*. The second part *(Monitoring and Modeling…)* seeks to improve methods for measuring changes in gravity, resistivity, self-potential and seismic properties caused by fluid production and injection, and to develop technology for integrated analyses of these data sets with conventional data, incorporating numerical reservoir modeling. In this way, more robust reservoir models can be developed to help optimize exploitation strategies, guide field management, and make geothermal electricity more competitive.

Part of this effort involves development of computer software suitable for conducting analyses of this type in combination with more conventional reservoir engineering studies. As a first step, we carried out a computational study of the feasibility of using these methods to characterize subsurface changes in geothermal systems. The specific objectives are (1) to devise a hypothetical but "typical" geothermal reservoir system, (2) to formulate a practical field exploitation strategy, (3) to perform a calculation of the behavior of the system during exploitation using the STAR reservoir simulator (Pritchett, 1995), (4) to use existing "postprocessors" (which compute microgravity and self-potential changes based on calculated underground reservoir changes) to assess these methods, and (5) to appraise the remaining survey techniques using prototype software as appropriate (Pritchett *et al*., 1998).

2. RESERVOIR DESCRIPTION

We consider the 9 km × 9 km area shown in Fig. 1. Fig. 2 shows a vertical cross-section (*CD* or *EF* in Fig. 1) through the center of the study volume, which extends to 3 km depth. The STAR grid consists of 8000 blocks (20 × 20 × 20), as indicated. Three rock formations (*Caprock, Aquifer* and *Basement*) are present, which differ in porosity and permeability. Both the *Aquifer* and *Basement* layers consist of "inner" and "outer" regions; the vertical permeabilities of the "inner" zones are relatively high. Other formation properties are uniform: rock grain density is 2.5 kg/liter, rock heat capacity is 1 kJ/kg-°C, and thermal conductivity is 3 W/m-°C. The dispersion scale (the quantity which, when multiplied by the local fluid velocity, yields the kinematic dispersion coefficient) is 50 m. Relative permeabilities are simple straight-line functions with residual water and steam saturations of 30% and 5% respectively. The vertical grid boundaries at ±4.5 km East and ±4.5 km North are impermeable and insulated. Pressure and temperature at the top grid surface (zero depth) are held at one bar and 20°C respectively. Most of the bottom surface (at 3 km depth) is impermeable, but an upward conductive heat flux of 0.18 W/m^2 (corresponding to a temperature gradient of 60°C/km) is imposed over the entire bottom surface. Furthermore, 100 kg of hot (350°C) water flows upward per second into the reservoir through a small central area (0.36 km^2) of the bottom surface.

To calculate the "natural state" of the system (conditions prior to human intervention), an initial temperature distribution was first imposed which is linear with depth, from 20°C at the surface to 200°C at 3 km depth (60°C/km gradient), with a corresponding hydrostatic initial pressure distribution. No steam is present initially. Next, a lengthy time-dependent STAR calculation was carried out representing 50,000 years of evolution – sufficient to reach a "natural state" that is steady for all practical purposes. Fig. 3 shows the final natural-state temperature distribution in the *CD* and *EF* (east-west and north-south) vertical planes (Fig. 1) which pass through the center of the area. The shaded region in Fig. 3 contains a flowing water/steam mixture; the remainder of the system is single-phase liquid. Heat transfer in the relatively impermeable *Basement* and *Caprock* layers is dominated by conduction, but

the permeable *Aquifer* layer is dominated by natural convection, with a pronounced temperature inversion. The highest temperatures are in the slender central upflow zone, and two-phase flow is likewise mainly confined to this region.

Next, starting with the "natural state" shown in Fig. 3 as initial conditions, a second STAR reservoir simulation was carried out which represents 10,000 days (~27 years) of 50 MW power production. Boundary conditions and formation properties are the same as for the natural-state calculation. Fluid is withdrawn from a region between 500 and 875 m depth underlying the "production area" shown in Fig. 1. Waste fluid is injected in the "injection area" between 625 and 750 m depth. Production wellhead pressures are maintained at 5.5 bars and the produced water/steam mixture is separated at 5.0 bars. The five-bar steam enters a single-flash condensing steam turbine and is expanded to condenser conditions (39°C; 0.07 bars) providing the motive power for the generator. The five-bar steam flow rate is maintained at 139 kg/s. Of the condensed steam (at 39°C), half is used by the evaporative cooling system; the rest is injected. The separated liquid (at 5 bars; 152°C) flows to an atmospheric flash tank where it is expanded to one atmosphere (100°C) and the steam and gas thereby evolved is vented. The remaining liquid is combined with the surplus condensate and injected.

Conditions in an east-west vertical cross-section (*AB* – see Fig. 1) which passes through the center of each wellfield are shown in Fig. 4 at the beginning *(natural state)* and the end *(10,000 days)* of this exploitation calculation. Temperatures have declined locally due to fluid injection, and the two-phase region has grown and migrated westward slightly. Steam saturations have also increased markedly. The total volume occupied by steam in the reservoir has more than doubled, from 0.11 km^3 under natural-state conditions to 0.27 km^3 after 10,000 days.

3. CHANGES IN SURFACE MICROGRAVITY

Next, STAR's "microgravity" postprocessor was used to calculate the gravity changes at the earth surface which are caused by the redistributions of underground fluid mass that result from production and injection. The postprocessor carries out spatial integrations of Newton's Law of Gravitation over the STAR grid volume at each time-level of interest for various points on the ground surface. Large gravity disturbances are confined to the general vicinity of the production and injection wells. Fig. 5 shows the spatial distributions of ground-surface microgravity change at 2000, 5000 and 10,000 days along east-west line *AB* (Fig. 1) which passes through the wellfields.

Gravity declines near the production wells due to steam volume increase, eventually approaching 1000 μgal reduction (1 μgal ≡ 10^{-8} m/s^2). A second, positive anomaly (smaller, but > 100 μgal) near the injection wells is caused by cooling and fluid densification. Changes less than 10 μgal can be identified by modern survey methods; computed disturbances are between one and two orders of magnitude larger. Detectable signals should appear during the first few months of field operation.

4. CHANGES IN SEISMIC PROPERTIES

Seismic techniques for monitoring operating geothermal fields include reflection surveys, refraction surveys, vertical seismic profiling and crosshole surveys. Changes in such surveys will be due to some combination of temporal changes in seismic velocities, reflections, refractions, and attenuation. We have not yet developed a general-purpose "postprocessor" to predict seismic survey results based on reservoir simulations. As a first step, consider seismic velocity changes likely to be caused by underground temperature and steam saturation changes. The general approach is outlined by Stevens *et al.* (2000). Here, we only consider the "vertical travel time" – the time required for a vertical wave from great depth to reach the surface. Fig. 6 shows the computed changes in vertical travel time along line *AB* (Fig. 1) after 2000, 5000 and 10,000 days. The principal feature is a growing region of reduced travel times near the injection wells resulting from compressibility decreases due to reservoir cooling. Smaller disturbances are also discernable associated with the production wells. In the production area, travel time changes include increases due to boiling of all-liquid zones (compressibility increase) followed by decreases caused by production-induced pressure (and temperature) decline (compressibility reduction). These changes in travel time are small but could be observed in a carefully planned experiment. A travel time reduction of 14 ms (Fig. 6) would result in an apparent (fictitious) upward displacement of a basement reflector of about 60 meters in a reflection survey.

5. MODELING ELECTRICAL RESISTIVITY

The remaining geophysical survey techniques (DC resistivity, MT and SP) all depend on the actual underground changes in electrical properties, particularly resistivity. The STAR field exploitation simulation calculates underground changes in pressure, temperature and steam saturation (*e.g.* Fig. 4). The next task is to estimate the changes in underground electrical resistivity that will result from these thermodynamic changes, so that these calculated "actual" resistivity changes can be used to appraise the utility of the various electrical survey techniques. For this preliminary study, a very simple model was adopted for this purpose, which is linear in the volume fractions of the pertinent materials (rock, water and steam):

$$(1/R) = ([1-\varphi]/R_r) + (\varphi[1-S]/R_w) + (\varphi S/R_s)$$

where R is bulk resistivity, R_r, R_w and R_s are the resistivities of rock, water and steam respectively, φ is rock porosity, and S is steam saturation. Resistivities of rock and steam are very high (taken as 10^5 and 10^3 Ω-m respectively for the present work), so that the most important term is the one containing R_w. The liquid water was treated as a dilute (1000 ppm) NaCl brine for which the dependence of resistivity on temperature is well-known. Fig. 7 shows the changes in underground electrical resistivity calculated in this way in the *AB* east-west cross-section during field exploitation. Two regions of resistivity change are apparent (both involving increases in resistivity). The larger and shallower (resistivity increase up to a factor of 3.4) lies at the top of the production volume and is caused by boiling and steam saturation increase. The smaller and deeper (resistivity increase a factor of 1.7 or less) surrounds the injection volume and is caused by temperature decline.

It should be noted that the above model for resistivity is actually very conservative for forecasting resistivity increases caused by boiling. For example, in an isothermal region in which the steam saturation (S) changes from zero (all-liquid) to 0.67, the model predicts an increase in bulk resistivity of a factor of three. For comparison, Archie's Law, which is often used to correlate electrical resistivity with water volume

fraction, would predict an increase in resistivity of nearly an order of magnitude under the same circumstances.

Because of the relative geometric simplicity of the present hypothetical reservoir model, small-scale resistivity variations from point to point which occur in real heterogeneous geothermal reservoirs are not present, so that the computed geophysical survey anomaly patterns are smoother than is usually observed in practice. Also, cultural effects upon resistivity changes such as the influences of makeup well casings must be accounted for under practical circumstances.

6. DC RESISTIVITY SURVEY CHANGES

A prototype STAR "testbed" DC resistivity postprocessor was used to examine changes that might be observed using a conventional earth-surface Schlumberger DC resistivity array. The array was oriented east-west with a current electrode spacing of 1200 m and a voltage electrode spacing of 120 m, located at the center of the production area. Fig. 8 shows the electrode arrangement and the calculated "apparent resistivity" history that would theoretically be observed by the array. The apparent DC resistivity (the resistivity of a uniform unbounded half-space that would yield the same ratio of voltage to current) increases by about one-third during the exploitation period, from 3.7 Ω-m in the natural state to 5.0 Ω-m at 10,000 days. Shifts of this size are well within the capabilities of existing measurement technology, particularly since the present model for actual underground resistivity change is quite conservative.

7. CHANGES IN MAGNETOTELLURIC SURVEYS

Calculations were also performed (Wannamaker, 1999) to estimate changes which would be observable in MT surveys due to underground resistivity changes arising from field exploitation operations. Based on the above conservative model for underground resistivity changes, MT apparent resistivity increases by up to 40% in the neighborhood of the production zone, accompanied by impedence phase decreases up to 6° and changes in normalized magnetic field of 0.02. Parameter changes of these magnitudes should all be detectable using modern instrumentation and survey procedures.

8. EFFECTS ON SELF-POTENTIAL SURVEYS

Electrokinetic effects resulting from production operations can induce electrical potential changes at the earth surface that can be measured by repeat self-potential surveys. Electrokinetic potentials arise from the interaction of the "drag current" (the subsurface distribution of electric current induced by liquid flowing through rock) with the spatial distribution of electrical resistivity, resulting in a potential distribution according to Ohm's Law. Thus, changes in surface potential arise from both changes in the electrical resistivity distribution and changes in subsurface flow. A postprocessor has been developed for the STAR simulator to facilitate the calculation of electrokinetic effects which result from geothermal field evolution (Ishido and Pritchett, 1999). It uses a procedure based on Ishido and Mizutani's (1981) experimental work to estimate realistic coupling coefficients relating fluid velocities to underground electric current densities. The postprocessor was applied to the present problem to estimate the changes likely to be caused in the natural-state potential distribution by the production of 50 MW of geothermal electricity for 10,000 days.

Results are illustrated in Fig. 9 for the *AB* east-west section: the curves represent the increase in SP (millivolts) relative to the natural state at t = 2000, 5000 and 10,000 days. A substantial disturbance (~60 mV peak-to-trough) is already present at 2000 days and, in fact, disturbances of several tens of millivolts appear within just a few days after field operations begin. This abrupt initial disturbance arises from the sudden change in underground flow. Thereafter, the potential distribution evolves slowly in response to changing electrical resistivities. SP changes eventually exceed 150 mV amplitude. Disturbances of this magnitude should be fairly easy to characterize with careful SP surveys. Continuous SP monitoring at a few selected locations may also prove worthwhile, particularly at times when flow rates change.

9. SUMMARY

Reservoir simulations have been carried out describing the subsurface effects of operating a 50 MW geothermal power station. Calculations were also performed to estimate changes in quantities observable using geophysical survey techniques (gravity, seismic velocity, SP, DC resistivity and MT) caused by field exploitation operations. Results suggest that all five techniques can discern operations-induced changes in the reservoir. Of course, the applicability of any particular method is likely to be highly site-specific, but these calculations indicate that none of these techniques should be ruled out altogether. Two major disturbances take place in the reservoir: boiling near the production wells and cooling near the injection wells. Some surveys (gravity, DC resistivity, MT) appear to be more sensitive to the production region, whereas others (seismic, SP) are more responsive to the injection zone.

Software development along these general lines is continuing. Application of these techniques to real operating geothermal fields is planned in the near future.

ACKNOWLEDGEMENTS

NEDO supported this work as part of the "New Sunshine Project" sponsored by the Agency of Industrial Science and Technology (AIST) of the Japanese Ministry of International Trade and Industry (MITI).

REFERENCES

Ishido, T. and H. Mizutani (1981). Experimental and theoretical basis of electrokinetic phenomena in rock-water systems and its applications to geophysics, *J. Geophys. Res.*, Vol. 86, pp. 1763-1775.

Ishido, T. and J. W. Pritchett (1999). Numerical simulation of electrokinetic potentials associated with subsurface fluid flow. *J. Geophys. Res*. (in press).

Pritchett, J. W. (1995). STAR: A geothermal reservoir simulation system. *Proc. World Geothermal Congress 1995,* Florence, pp. 2959-2963.

Pritchett, J. W., J. L. Stevens, J. Combs and S. K. Garg (1998). *Utilization of Nonconventional Data Sets for Geothermal Reservoir Monitoring: A Computational Feasibility Study.* Maxwell Technologies Report No. MSD-DTR-98-16048.

Stevens, J.L., J.W. Pritchett, S.K. Garg, K. Ariki, S. Nakanishi and S. Yamazawa, (2000). Seismic methods for observing geothermal field evolution. *Proc. World Geothermal Congress 2000*, Japan (in press).

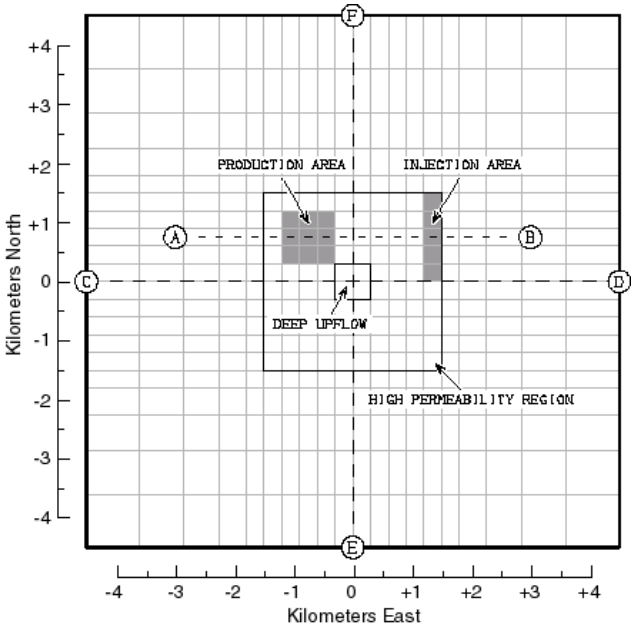

Figure 1. Area map showing locations of cross-sections *AB*, *CD* and *EF*, production and injection wellfields, regions of high permeability, and STAR computational grid spacing.

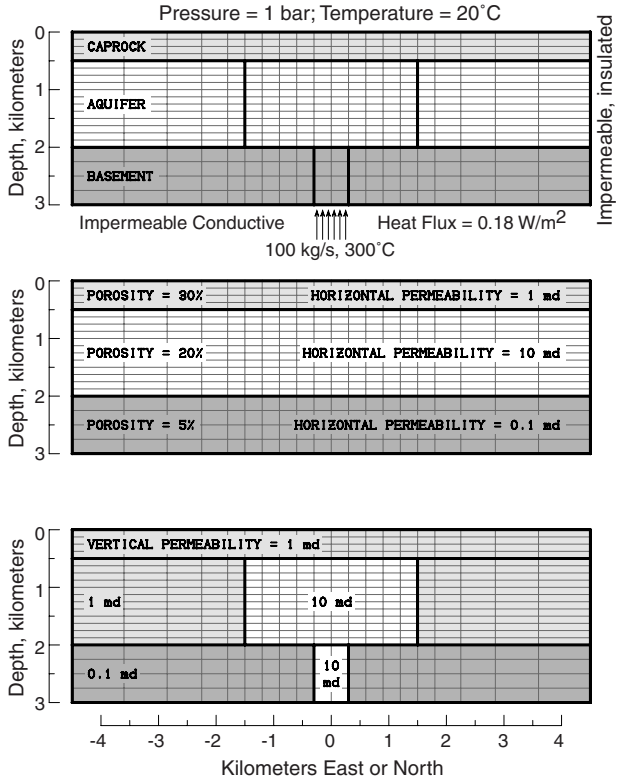

Figure 2. Vertical cross-sections *CD* and *EF* showing STAR grid spacing, boundary conditions, geological structure, and porosity and permeability distributions.

Wannamaker, P. E. (1999). *Magnetotelluric Simulation of Subsurface Resistivity Changes Due to Fluid Production from a Model Geothermal Reservoir.* Maxwell Technologies Report No. MTSD-DTR-99-16324.

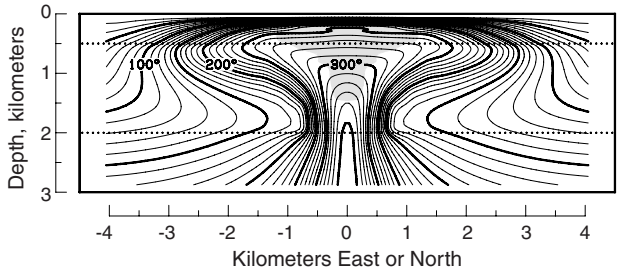

Figure 3. Natural-state temperatures (°C) in the *CD* and *EF* vertical planes (Figure 1) after 50,000 years of stabilization. Contour spacing: 10°C. Shaded area: two-phase flow region. Dotted lines delineate structural boundaries separating *Caprock, Aquifer* and *Basement* layers.

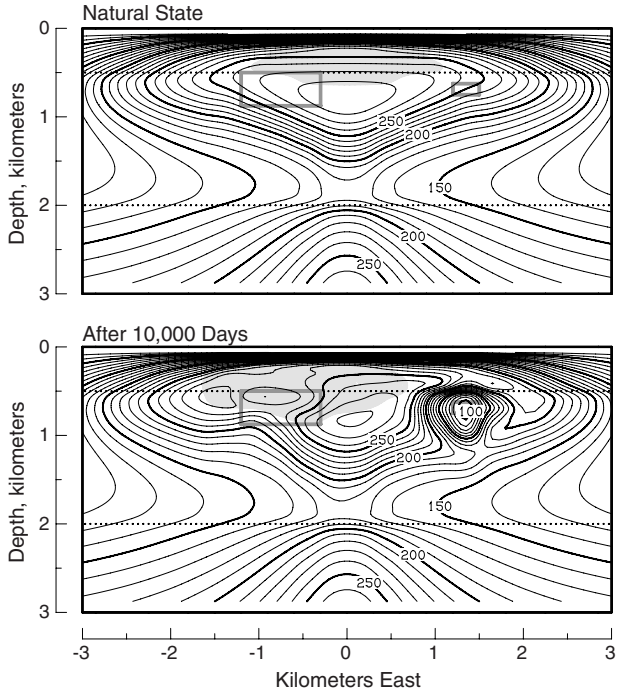

Figure 4. Effects of 10,000 days of field operation on underground temperatures (°C) in east-west *AB* vertical plane (Figure 1). Contour spacing: 10°C. Shading: two-phase flow. Rectangles: production and injection volumes.

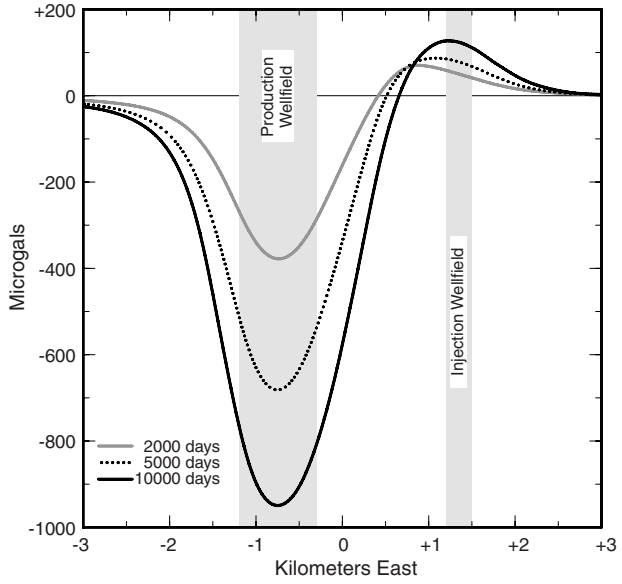

Figure 5. Changes in surface microgravity (μgal) relative to natural state along line *AB* (Figure 1).

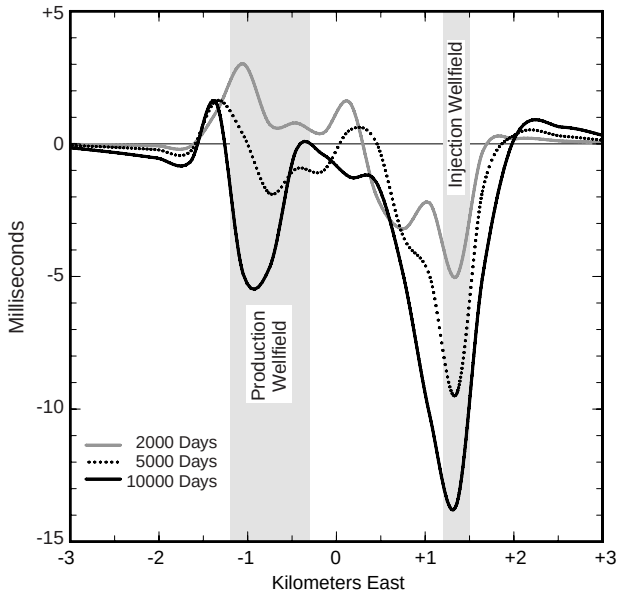

Figure 6. Changes in vertical seismic travel time (ms) relative to the natural state along line *AB* (Figure 1).

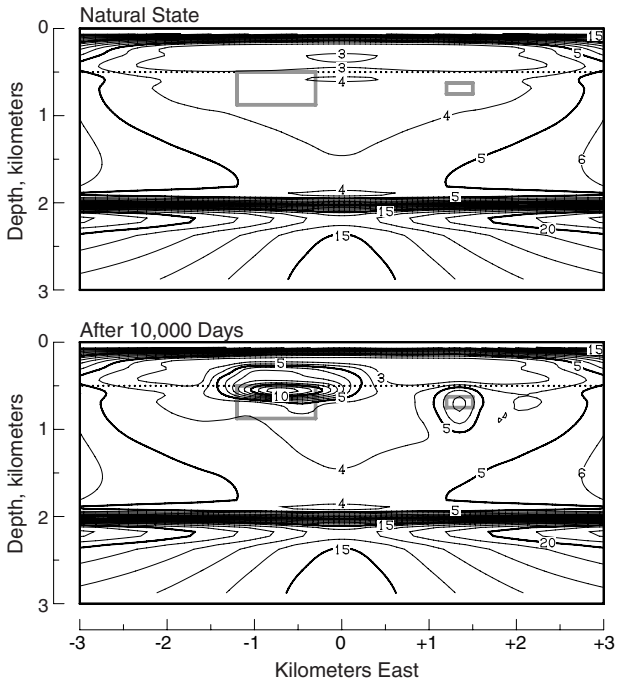

Figure 7. Effects of 10,000 days of field operation on underground electrical resistivity (Ω-m) in east-west *AB* vertical plane (Figure 1). Contour spacing: 1 Ω-m. Rectangles: production and injection volumes.

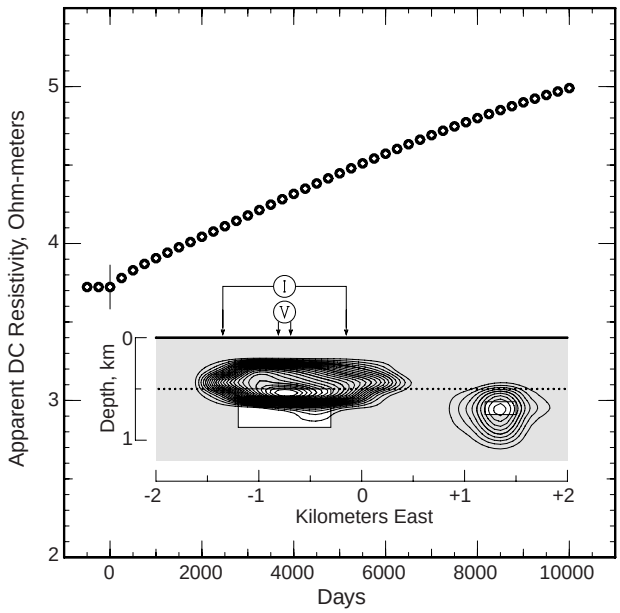

Figure 8. Apparent DC resistivity (Ω-m) vs. time at production wellfield center as measured by Schlumberger array. Inset: array geometry; contours show resistivity increase relative to natural state (10%, 20%, 30% …).

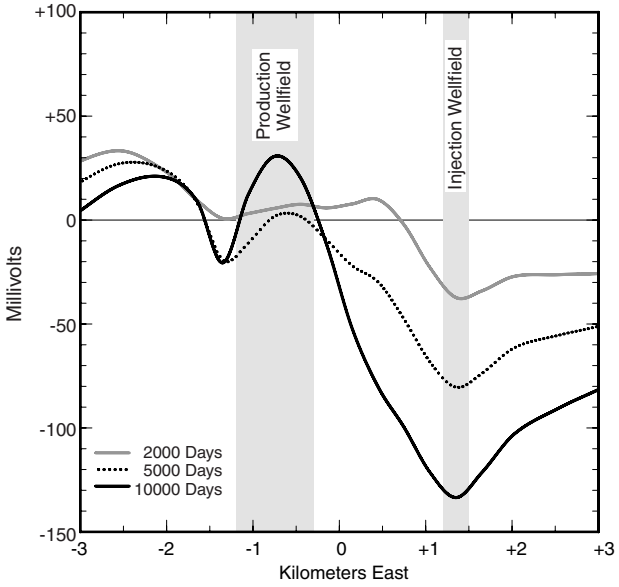

Figure 9. Changes in ground surface self-potential (mV) relative to the natural state along line *AB* (Figure 1).